A Rapid, Low-Cost, and Scalable Technique for Printing State-of-the-Art Organic Field-Effect Transistors

*Inés Temiño, Freddy G. Del Pozo, M. R. Ajayakumar, Sergi Galindo, Joaquim Puigdollers, and Marta Mas-Torrent**

In the last few years exciting advances have been achieved in developing printing techniques for organic semiconductors, and impressive mobility values have been reported for the resulting organic field-effect transistors (OFETs). However, not all these techniques are scalable and some of them require additional crystallization steps. This study reports on the fabrication of OFETs employing blends of four benchmark organic semiconductors with polystyrene and demonstrates that applying the same formulation and experimental conditions for printing them, highly reproducible and uniform crystalline films exhibiting high OFET performance are successfully achieved. It is noted that the mobility values achieved here are not the highest reported for the studied materials; however, they are state-of-the-art values and could be regarded as exceptional considering the low cost and fast speed of the fabrication process involved here.

1. Introduction

The first report of an organic field-effect transistor (OFET) based on a small conjugated molecule was published over thirty years ago.[1] This discovery prompted investigations into the fundamental physical aspects of these devices employing evaporated semiconductors, such as pentacene and sexithiophene. However, in order to exploit these devices in real applications it was soon realized that high performing materials should be stable and soluble in order to be processed from low-cost solution techniques. This shifting perspective caused a huge boost in the synthesis of novel organic semiconductors. Nowadays, there is a vast library of known materials that have been employed as active components in OFETs, and some of them meet the desired requirements for low-cost applications.[2,3] Now, the challenge lies in engineering processing techniques that could give rise to highly crystalline and homogenous semiconducting films potentially resulting in reproducibly high mobility devices.[4–6] To make organic electronics competitive with their inorganic counterparts and to promote a competitive market entry, such techniques must be simple, cheap, and compatible with upscaling and high throughput processes such as roll-to-roll. In the last few years, exciting advances have been achieved in this direction and OFETs fabricated utilizing different solution deposition techniques have been reported exhibiting impressive mobility values.[7–20] However, not all these techniques are scalable and some of them require additional crystallization steps (i.e., vapor or temperature annealing processes). Importantly, most reported processing techniques are not universal as they are often adapted for a particular organic semiconductor. Recently, we reported a solution-shearing technique, namely bar-assisted meniscus shearing (BAMS), of an organic semiconductor blend based on the small semiconducting molecule dibenzo-tetrathiafulvalene (DB-TTF) and the insulating polymer polystyrene (PS). This technique resulted in highly crystalline thin films that showed ideal OFET characteristics.[21,22] The question raised at this point was if the BAMS technique could be extended to other organic semiconductors. Here, we report on the fabrication of OFETs employing blends of four benchmark organic semiconductors with PS and we demonstrate that applying the same formulation and experimental conditions for printing them, highly reproducible and uniform crystalline films exhibiting high OFET performance are successfully achieved. We note that the mobility values achieved here are not the highest reported for the studied materials, however, they are state-of-the-art values and could be regarded as exceptional considering the low cost and fast speed of the fabrication process involved here.

I. Temiño, Dr. F. G. Del Pozo, Dr. M. R. Ajayakumar, Dr. S. Galindo, Dr. M. Mas-Torrent
Institut de Ciència de Materials de Barcelona (ICMAB-CSIC) and Networking Research Center on Bioengineering Biomaterials and Nanomedicine (CIBER-BBN)
Campus, UAB, 08193 Bellaterra, Spain
E-mail: mmas@icmab.es
Dr. F. G. Del Pozo
Universidad Técnica de Ambato
Av. Colombia y Chile, Ambato EC180105, Tungurahua, Ecuador
Dr. J. Puigdollers
Dept. Enginyeria Electrònica
Universitat Politècnica Catalunya
C/Jordi Girona, 31, 08034 Barcelona, Spain

DOI: 10.1002/admt.201600090

2. Results and Discussion

The organic semiconductors (OSCs) chosen for this study have been 6,13-bis(triisopropylsilylethinyl)pentacene (TIPS-PEN), 2,8-difluoro-5,11-bis(triethylsilylethynyl)anthradithiophene (diF-TES-ADT), 2,7-dioctyl[1]benzothieno[3,2-b][1]benzothiophene (C8-BTBT), and dithiophene-tetrathiafulvalene (DT-TTF) (**Figure 1**a). DT-TTF was synthesized in our laboratory

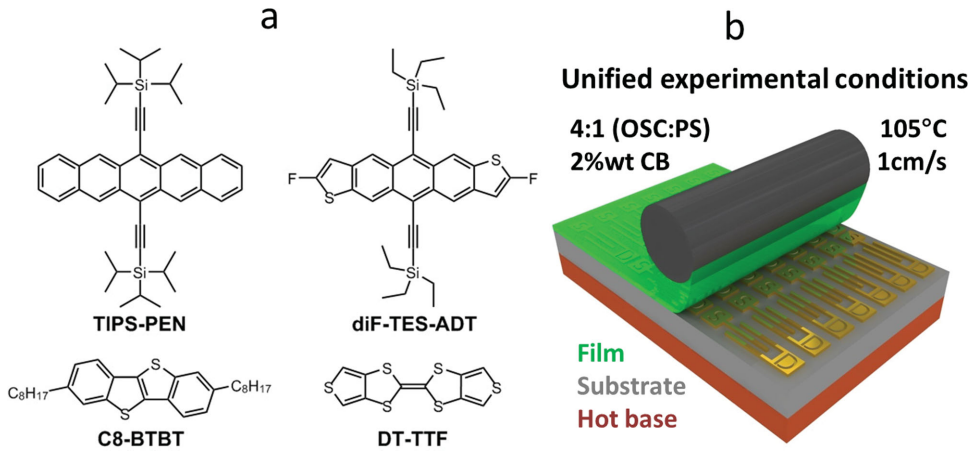

Figure 1. a) Molecular structures of the organic semiconductors used. b) Schematic illustration of the BAMS coating technique together with the experimental conditions used.

as previously reported[23] and the rest of semiconductors were used as received. All these materials belong to different families of OSCs and have been reported to be excellent candidates for OFETs.[9,14,20,24,25]

The use of solution inks based on blends of OSCs and inert polymers has been shown to be a promising route to gain material processability and film homogeneity.[26,27] Solutions of the above-mentioned semiconductors with PS with molecular weight M_w = 10000 g mol^{-1} (PS10000) in a ratio 4:1 in 2 wt% in chlorobenzene were prepared. Thin crystalline films were printed by following the previously reported BAMS methodology.[21] Bottom gate bottom contact devices that consisted of Si/SiO_2 substrates with patterned Cr/Au electrodes were used for TIPS-PEN, diF-TES-ADT, and DT-TTF. Bare gold electrodes and electrodes treated with a self-assembled monolayer (SAM) of pentafluorobenzenethiol (PFBT) were tested. The substrates were placed on the coating bed at 105 °C and a smooth bar was located 300 µm above the sample. About 20 µL of the blend solution heated at the same temperature as the bed coater were deposited between the substrate and the bar, and immediately after that, the bar was sheared at a speed of 1 cm s^{-1}. In the case of C8-BTBT the same printing procedure was followed but the films were prepared on bare Si/SiO_2 and top MoO_3/Au contacts evaporated through a shadow mask were fabricated. Such contacts ensure efficient charge injection into the material, which is otherwise more difficult to realize with gold electrodes due to the very low lying highest occupied molecular orbital level of this molecule (≈ −5.5 eV).[28] It should be highlighted that the complete experimental procedure, which is shown in Figure 1b, was carried out under ambient conditions. Notice that this process leads to the formation of dry films since the solvent is evaporated as soon as the bar is sheared. Similar films can be also obtained using solvents such as toluene or tetraline, although then the temperature is adjusted depending on the boiling point and vapor pressure of the solvent to guarantee the immediate evaporation of the solvent.

Previously, it was reported that the use of gold source and drain electrodes modified with the fluorinated PFBT SAM improved dramatically the crystallization of TIPS-PEN and diF-TES-ADT in spin coated films.[10,29–31] It was observed that due to a contact-induced crystallization, crystals grew from the contacts and extended 10 µm into the transistor channel. However, in thin films fabricated by plate-shearing at 1.5 mm s^{-1}, PFBT SAMs disrupted the formation of spherulitic crystalline structures.[10] Thus, Niazi et al. concluded that strongly interacting contacts were not suitable for achieving the larger domains typically obtained by solution-shearing techniques. In contrast, in our shearing based technique we found that PFBT SAMs lead to more homogenous and interconnected crystallites in the TIPS-PEN and diF-TES-ADT films, which in turn results in higher mobility OFET devices (Figure S1, Supporting Information). Remarkably, such crystalline domains extend along the whole channel (L is in the range 25–100 µm). This discrepancy with previous reported results can be attributed to the higher speed of our process (i.e., one order of magnitude faster) and maybe the less confinement of the solution when a bar is used instead of a plate. These factors might be responsible for the fact that the treated electrodes assist the materials crystallization. On the other hand, the crystallization of DT-TTF films is not influenced by the treatment of the electrodes.

In **Figure 2**, the polarized optical microscopy images of the prepared films are shown, where clear uniform crystalline domains can be observed. TIPS-PEN, diF-TES-ADT, and C8-BTBT OSCs grow forming spherulitic films with no preferential orientation relative to the shearing direction. On the contrary, DT-TTF films are formed by several millimeter long domains grown along the shearing direction. The film morphologies and thicknesses were further characterized using atomic force microscopy (Figure S2, Supporting Information). The surface roughness of the films was estimated to be 3.3, 1.2, 6.0, and 11.3 nm for TIPS-PEN, diF-TES-ADT, C8-BTBT, and DT-TTF films, respectively, pointing out the smoothness of the films. In addition, the total thickness of the blended films was estimated to be around ≈20 nm for TIPS-PEN and diF-TES-ADT, while C8-BTBT and DT-TTF films were estimated to be 43 and 13 nm, respectively.

In order to gain information about the crystallinity of the films, they were characterized by X-ray powder diffraction (Figure S3, Supporting Information). In all cases, clear sets of diffraction peaks were observed, indicative of their high degree

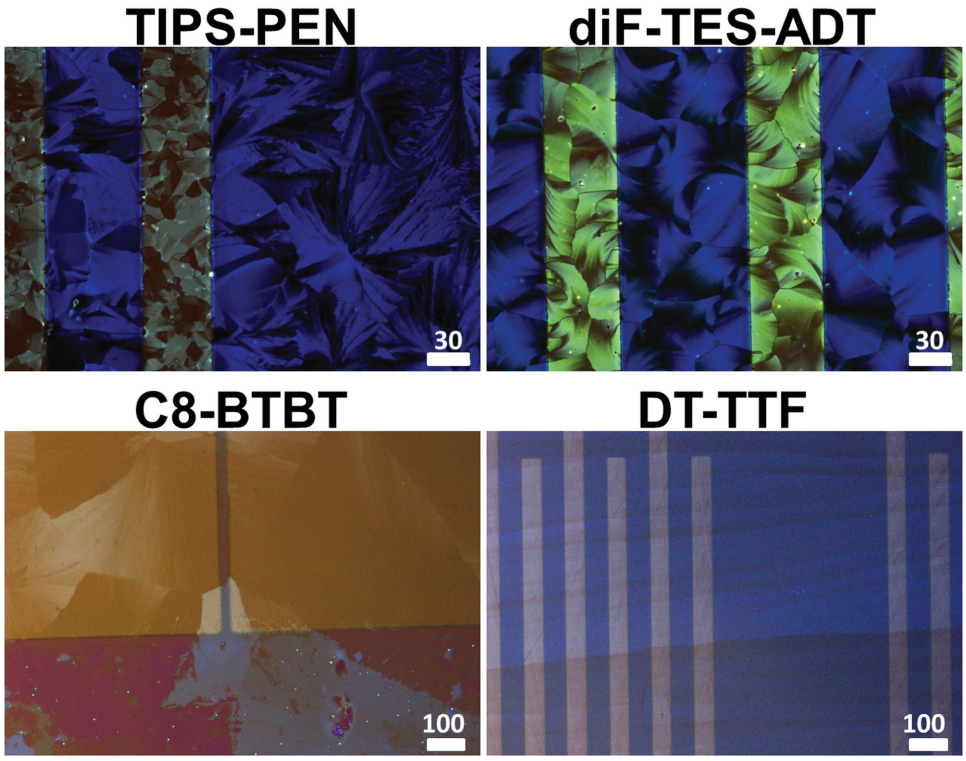

Figure 2. Optical polarized microscopy images of TIPS-PEN, diF-TES-ADT, C8-BTBT, and DT-TTF thin films. In the case of TIPS-PEN and diF-TES-ADT the electrodes are treated with a PFBT SAM. Scale bar: 30 and 100 μm for the upper and lower images, respectively.

of crystallinity. The crystal patterns of TIPS-PEN and diF-TES-ADT are in agreement with the previous triclinic phases reported for these materials, where the molecules adopt a 2D π-stack.[32–35] On the other hand, the crystal phase of C8-BTBT and DT-TTF correspond to their known monoclinic crystal structures in which molecules arrange in a herringbone configuration.[25,36] The observation of only *(00l)* type reflections for all the studied OSCs suggests that the crystallites in the films are highly oriented with the *ab* plane parallel to the substrate, which is the most favorable scenario for charge transport since corresponds to the plane where intermolecular electronic interactions exist. X-ray photoelectron spectroscopy measurements were also performed to analyze the film chemical composition at the surface (Figure S4, Supporting Information). In all the thin films, the contents of Si (for TIPS-PEN) or S (for diF-TES-ADT, C8-BTBT, and DT-TTF) demonstrated the presence of the OSC at the top film surface. By analyzing the distribution of these elements at different film depths using time-of-flight secondary ion mass spectrometry (ToF-SIMS) it was verified that there is a vertical phase separation where an OSC layer is formed on top of a PS layer (Figure S5, Supporting Information).

The devices were electrically measured under ambient conditions. Typical OFET transfer characteristics and mobility profiles of devices using PS blends of TIPS-PEN, diF-TES-ADT, C8-BTBT, and DT-TTF are illustrated in **Figures 3** and **4**, respectively, while the output characteristics are shown in Figure S6 (Supporting Information). In all cases, the mobility dependence with the gate voltage is quite small, indicative of a pristine organic semiconductor/dielectric interface. The box chart of **Figure 5** collects the mobility values of all the measured devices (notice that this statistical analysis has been performed using data from OFETs prepared on different areas of one film but also on different substrates, to ensure film homogeneity and device-to-device reproducibility). For TIPS-PEN, a very small hysteresis was observed between the forward and reverse V_{SD} and V_{SG} sweeps (in the output and transfer characteristics, respectively), again in agreement with a neat semiconductor/dielectric interface. Furthermore, the measured devices exhibited a high average and maximum field-effect mobility of μ_{FE} = 1.6 and 2.1 cm^2 V^{-1} s^{-1}, respectively, as well as a low threshold voltage of about V_{th} = –0.9 V (average) extracted in the saturation regime. A similar picture is found for diF-TES-ADT based devices, for which the average field-effect mobility found is of μ_{FE} = 1.3 cm^2 V^{-1} s^{-1} and the maximum of 1.9 cm^2 V^{-1} s^{-1}. The average threshold voltage extracted is V_{th} = +0.8 V. Note that for both semiconductors devices turn on at a gate voltage near to 0 V, and afterward the channel current is enhanced by 7 orders of magnitude (on/off ratio ≈10^7). Also, ideal output characteristics showing no significant injection problems are observed (Figure S6, Supporting Information). In the case of C8-BTBT an average field-effect mobility of μ_{FE} = 0.26 cm^2 V^{-1} s^{-1} was extracted in the saturation regime, while the maximum value was found to be 0.71 cm^2 V^{-1} s^{-1}. A couple of devices with outstanding mobility (μ_{FE} about 1.6 cm^2 V^{-1} s^{-1}) were measured; however, they were considered as outliers and thus they were not included in the data set for statistical calculations in Figure 5. An average threshold voltage of V_{th} = –29 V was found. This value is in agreement with other reported studies performed with this organic semiconductor.[37] Finally

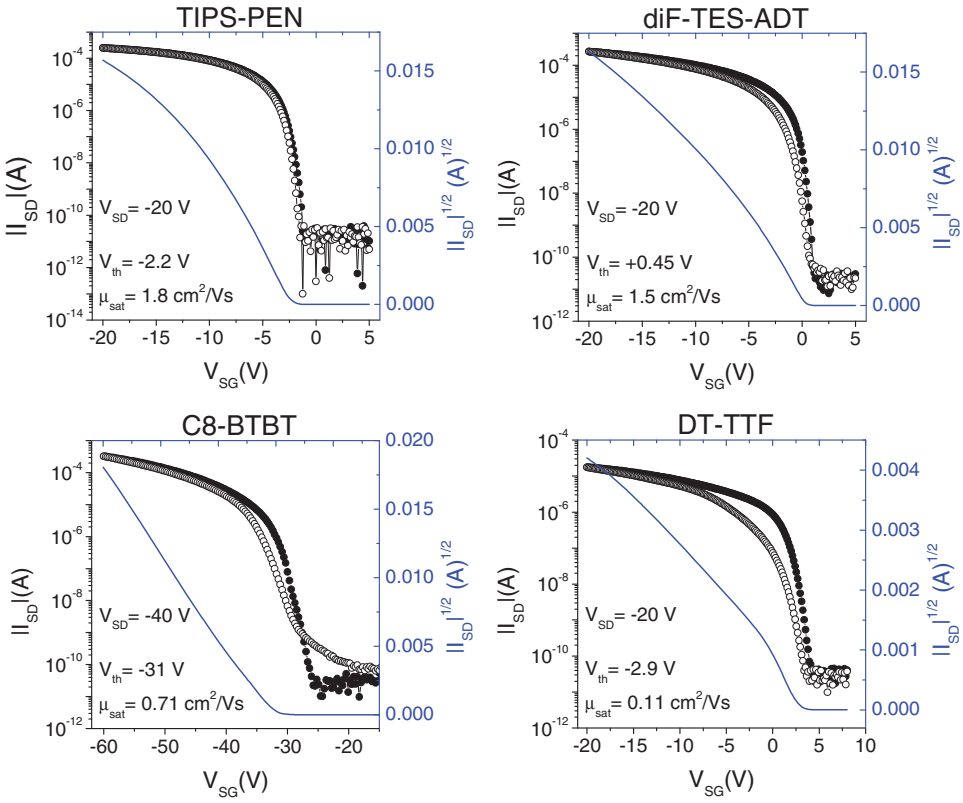

Figure 3. Transfer characteristics in the saturation regime and extraction of field-effect mobility and threshold voltage of typical TIPS-PEN, diF-TES-ADT, C8-BTBT, and DT-TTF blended films prepared by BAMS. Closed symbols correspond to forward, while open symbols correspond to reverse sweeps of gate voltages.

DT-TTF based devices showed an average threshold voltage of V_{th} = +3.9 V. The average and maximum field-effect mobility measured were μ_{FE} = 0.10 and 0.13 cm^2 V^{-1} s^{-1}, respectively, which is as high as the mobilities reported for single crystals of this DT-TTF phase.[25] Devices based on these last two semiconductors showed an on/off ratio on the order 10^6–10^7. It should be highlighted here that only DT-TTF devices showed electrical anisotropy, giving mobilities of around one order of magnitude higher when the device channel length was parallel to the shearing direction than when it was perpendicular to it (see Figure S7 in the Supporting Information). The rest of the materials were fully isotropic.

As it can be seen in the box chart of Figure 5, there is not a large dispersion between the mobility values extracted for all devices of each semiconductor, which indicates there is a low device-to-device variation thanks to high uniformity of the films obtained with the BAMS fabrication process. Moreover, the mobility profiles in Figure 4 show low gate voltage dependence. Such field-independent device mobility is in agreement with a high crystalline quality of all the solution-processed semiconducting films.

The mobility values achieved for the studied OSCs with BAMS technique are among the highest values reported for these materials. **Table 1** collects the recent results reported for the fabrication of OFET devices based on TIPS-PEN, diF-TES-ADT, C8-BTBT, and DT-TTF employing techniques compatible with roll-to-roll. The experimental conditions including the velocity of the coating process are shown together with the OFET mobility reached. Most of the efforts on engineering high-performing OFET devices have been placed on TIPS-PEN and diF-TES-ADT. Both materials have been carefully investigated by the technique developed by Bao and co-workers consisting in the confinement of the OSC solution between a heated phenyltrichlorosilane SiO_2 modified substrate and a top silicon wafer plate functionalized with a monolayer of octadecyltrichlorosilane.[38] The shearing plate drags the solution across the substrate keeping the bulk of the solution between the plate and the substrate with only the evaporation front exposed. With this methodology mobility values of up to 4.6 and 6.7 cm^2 V^{-1} s^{-1} have been found for TIPS-PEN and diF-TES-ADT, respectively.[10,14] For TIPS-PEN, mobilities up to 11 cm^2 V^{-1} s^{-1} were also reported when plates with patterned micropillars were used, although in that case the resulting films were very anisotropic.[9] However, in all these works, the coating speed was at least half of the one used here, and typically, of one order of magnitude lower. Only in two cases these materials have been printed with processes of comparable speed as BAMS, but not only the mobility values achieved were lower but also either a long post-treatment step was required[7] or a semiconducting polymer was used as binder.[13] The C8-BTBT semiconductor has been extensively studied and excellent mobility values have been reported for this material, although in most of the cases it was processed by spin-coating based techniques and, furthermore, slow post-annealing processes

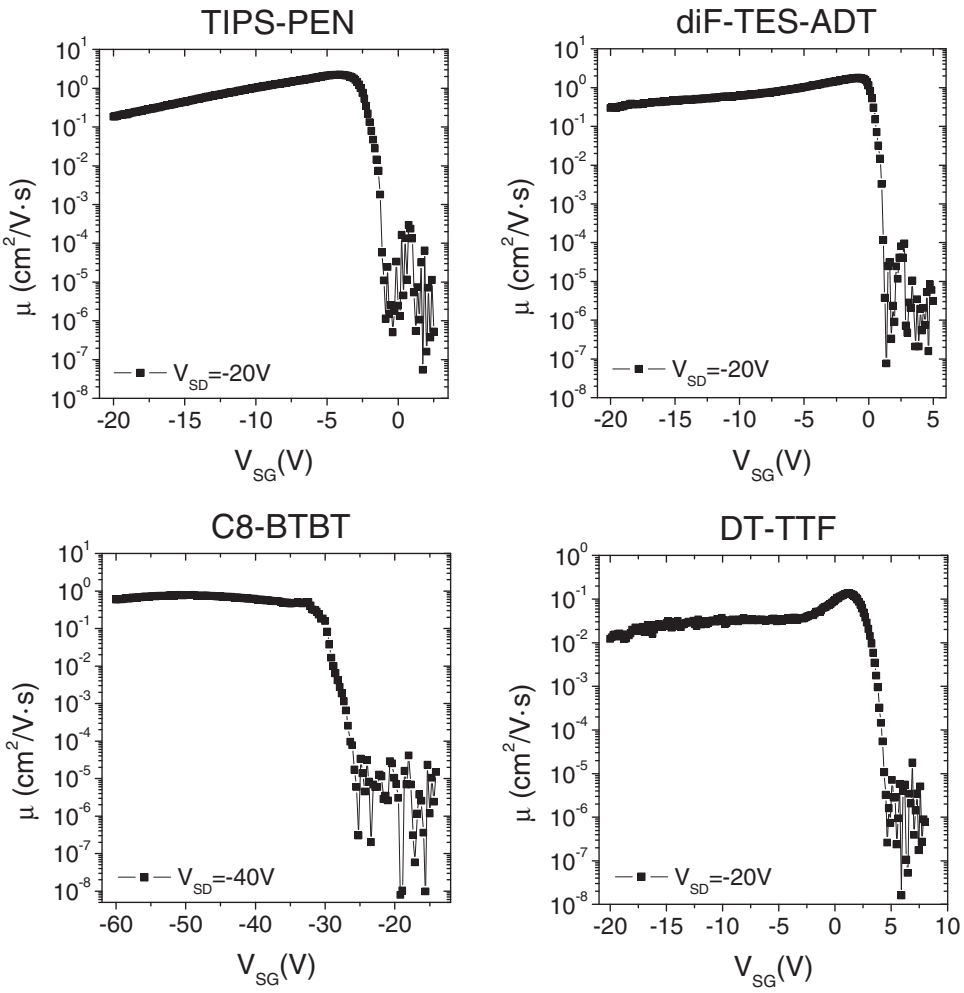

Figure 4. Mobility profiles for saturation regime as a function of gate voltage for typical TIPS-PEN, diF-TES-ADT, C8-BTBT, and DT-TTF blended films.

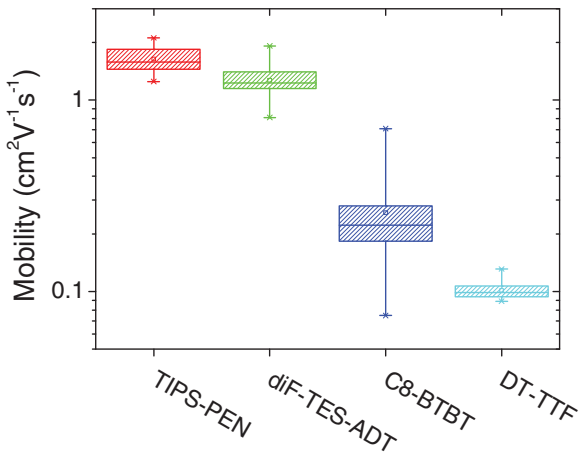

Figure 5. Box-plot for field-effect mobility values for TIPS-PEN, diF-TES-ADT, C8-BTBT, and DT-TTF devices extracted in the saturation regime. For each data set, the box includes all the data between the first and the third quartile, the line inside each box is the second quartile or the median, and the square represents the mean value. The extremes of the whiskers are the maxima and minima data found.

were often applied.[19,20,37,39] As reference, a few works have been included in Table 1 where printed C8-BTBT devices were reported, although the techniques used there are not readily scalable since they mainly consist of a crystallization process by drop casting.[17,18,40] Finally, high mobility films of DT-TTF were previously fabricated by zone-casting, a far too slow technique for applications.[41] Considering all the above facts, it is noticeable that the OFET performances reported here can be regarded as state-of-the-art, especially taking into account the simplicity and low cost of the technique employed combined with the high speed of the process.

3. Conclusions

In summary, four benchmark organic semiconductors have been successfully printed employing a unique formulation and the bar-assisted meniscus shearing (BAMS) technique. Homogenous films exhibiting a high degree of crystallinity were realized applying a remarkably high coating speed and without any post-treatment thanks to the combination of the BAMS technology with the blending of the organic semiconductors with polystyrene,

Table 1. Comparison of reported results of TIPS-PEN, diF-TES-ADT, C8-BTBT, and DT-TTF based OFETs processed by roll-to-roll compatible techniques, highlighting some of the experimental details as the coating speed (v), the use of post thermal treatments, the binder used (if any), and the maximum (max.) and average (av.) mobility values achieved. nr stands for not reported. Binders: PαMS (Poly(alpha-methylstyrene)), PS (Polystyrene), PTAA (poly[bis(4-phenyl)-(2,4,6-trimethylphenyl)amine]).

OSC	Experimental method details	V[mms^{-1}]	Binder	μ[cm^{2}V^{-1}s^{-1}]		Ref.
				av.	max.	
TIPS-PEN	Horitzontal dipping, post-treatment at 100 °C for 60 min	15	PαMS	0.15	0.22	[7]
	Shearing plate 8° tilt, substrate and plate chemically modified 90 °C	4	–	1.68	2.7	[8]
	Shearing plate 8° tilt, substrate and plate chemically modified, plate with patterned micropillars, 135 °C	0.6	–	8.1	11	[9]
	Shearing plate 8° tilt, substrate and plate chemically modified, 70 °C	≈1	PαMS	nr	4.6	[10]
	BAMS	10	PS	1.6	2.1	
diF-TES-ADT	Doctor Blade coating in a glovebox, drying, and post-treatment at 100 °C for 10 min and cooling to 65 °C	10–20	PTAA	0.68	1.6	[13]
	Shearing plate 8° tilt, substrate and plate chemically modified, 70 °C	≈1	PαMS	nr	3.6	[10]
	Shearing plate 8° tilt, substrate and plate chemically modified, dual solvent, 100 °C	0.5	PS	nr	6.7	[14]
	BAMS	10	PS	1.3	1.9	
C8-BTBT	Single crystal growth by oriented crystallization on inclined substrate, solution dries for 5 h at 50 °C in vacuum	–	–	nr	5	[17]
	Drop casting on a patterned substrate with wettable and unwettable regions	–	–	0.53	nr	[18]
	Drop casting on a patterned substrate with lyophilic and lyophobic regions	–	–	7.9	nr	[40]
	BAMS	10	PS	0.26	1.6	
DT-TTF	Zone-casting at 60 °C	0.03	–	nr	0.17	[41]
	BAMS	10	PS	0.10	0.13	

which promotes processability and an enhanced crystallization of the semiconductor. Such films reveal very high and reproducible field-effect mobility values. The potential of implementing organic semiconducting molecules in real devices seems to be a close reality taking into account the excellent performance of the devices achieved and that they can be fabricated using a cheap, simple, and fast technique compatible with roll-to-roll processes.

4. Experimental Section

Sample Preparation: TIPS-PEN, diF-TES-ADT and both C8-BTBT and PS10000 were purchased from Ossila, Lumtec, and Sigma-Aldrich, respectively, and used without further purification. DT-TTF was synthesized in our laboratory following the previously reported procedure.[23] Solutions of these OSCs and PS10000 2 wt% in chlorobenzene were prepared by mixing solutions at a volume ratio of 4:1 OSC:PS. The substrates employed for solution coating consisted of Si/SiO_2 (200 nm SiO_2) from Si-Mat with photolithography patterned interdigitated electrodes of 4 nm of Cr and 40 nm of gold, deposited by thermal evaporation. The channel lengths varied from 25 to 100 μm and channel width/length ratio was always set to 100. However, for C8-BTBT top contact devices that consisted of 7 nm of MoO_3 and 35 nm of gold were thermally evaporated through a shadow mask giving devices with channel lengths from 30 to 100 μm and channel width of 4 mm. Before the active-layer deposition, substrates were cleaned by high performance liquid chromatography quality acetone and isopropanol and then dried under nitrogen. When the gold surface was chemically modified, the substrates were first cleaned using ultraviolet ozone for 25 min and then immersing them in a 15×10^{-3} M solution of PFBT in isopropanol for 15 min. Finally, the substrates were rinsed with pure isopropanol. The OSC blend solutions were sheared with a home-designed bar coater in which a smooth cylindrical bar was positioned ≈300 μm above the substrates which was then sheared at speed of 1 cm s^{-1}. The substrates were kept at 105 °C during the coating process. Note that all solution preparation and device processing steps were carried out under ambient conditions.

Device Characterization: Electrical measurements were performed using an Agilent B1500A semiconductor device analyzer connected to the samples with a Karl SÜSS probe station, at ambient conditions. The field-effect mobility in the saturation regime was extracted using the relationship

$$\mu_{FE,sat} = \frac{2L}{WC} \times \left(\frac{\partial \sqrt{|I_{SD,sat}|}}{\partial V_{SG}} \right)^2 \quad (1)$$

where C is the insulator capacitance per unit area, and W and L are the width and length of the channel, respectively.

Supporting Information

Supporting Information is available from the Wiley Online Library or from the author.

Acknowledgements

This work was mainly funded by the ERC StG 2012-306826 e-GAMES and ERC PoC 2014-640120 LAB-TECH projects. The authors also thank the Networking Research Center on Bioengineering, Biomaterials, and Nanomedicine (CIBER-BBN), the DGI (Spain) project BE-WELL CTQ2013-40480-R and ENE2014-56237-C4, the Generalitat de Catalunya (2014-SGR-17) and the Spanish Ministry of Economy and

Competitiveness, through the "Severo Ochoa" Programme for Centres of Excellence in R&D (SEV-2015-0496). The authors would like to thank the ICTS "NANBIOSIS", more specifically to the Nanotechnology Platform, unit of CIBER-BBN at the Institute for Bioengineering of Catalonia (IBEC) for their assistance in ToF-SIMS analyses. I.T. is enrolled in the Materials Science PhD Program of Universitat Autònoma de Barcelona and acknowledges FPU fellowship from the Ministery. F.G.D.P. thanks Universidad Técnica de Ambato and Secretaría de Educación Superior, Ciencia, Tecnología e Innovación for funding through a doctoral scholarship "Convocatoria abierta 2010."

Received: May 18, 2016
Revised: May 25, 2016
Published online: June 15, 2016

[1] G. Horowitz, D. Fichou, X. Peng, Z. Xu, F. Garnier, *Solid State Commun.* **1989**, *72*, 381.
[2] M. Mas-Torrent, C. Rovira, *Chem. Soc. Rev.* **2008**, *37*, 827.
[3] W. Wu, Y. Liu, D. Zhu, *Chem. Soc. Rev.* **2010**, *39*, 1489.
[4] Y. Xu, C. Liu, D. Khim, Y.-Y. Noh, *Phys. Chem. Chem. Phys.* **2015**, *17*, 26553.
[5] G. Schweicher, Y. Olivier, V. Lemaur, Y. H. Geerts, *Isr. J. Chem.* **2014**, *54*, 595.
[6] Y. Diao, L. Shaw, Z. Bao, S. C. B. Mannsfeld, *Energy Environ. Sci.* **2014**, *7*, 2145.
[7] B. Park, H. G. Jeon, J. Choi, Y. K. Kim, J. Lim, J. Jung, S. Y. Cho, C. Lee, *J. Mater. Chem.* **2012**, *22*, 5641.
[8] G. Giri, S. Park, M. Vosgueritchian, M. M. Shulaker, Z. Bao, *Adv. Mater.* **2014**, *26*, 487.
[9] Y. Diao, B. C.-K. Tee, G. Giri, J. Xu, D. H. Kim, H. A. Becerril, R. M. Stoltenberg, T. H. Lee, G. Xue, S. C. B. Mannsfeld, Z. Bao, *Nat. Mater.* **2013**, *12*, 665.
[10] M. R. Niazi, R. Li, M. Abdelsamie, K. Zhao, D. H. Anjum, M. M. Payne, J. Anthony, D.-M. Smilgies, A. Amassian, *Adv. Funct. Mater.* **2016**, *26*, 2371.
[11] T. Sakanoue, H. Sirringhaus, *Nat. Mater.* **2010**, *9*, 736.
[12] H. Yoo, H. H. Choi, T. J. Shin, T. Rim, K. Cho, S. Jung, J.-J. Kim, *Adv. Funct. Mater.* **2015**, *25*, 3658.
[13] A. Pierre, M. Sadeghi, M. M. Payne, A. Facchetti, J. E. Anthony, A. C. Arias, *Adv. Mater.* **2014**, *26*, 5722.
[14] M. R. Niazi, R. Li, E. Qiang Li, A. R. Kirmani, M. Abdelsamie, Q. Wang, W. Pan, M. M. Payne, J. E. Anthony, D.-M. Smilgies, S. T. Thoroddsen, E. P. Giannelis, A. Amassian, *Nat. Commun.* **2015**, *6*, 8598.
[15] S. Hunter, J. Chen, T. D. Anthopoulos, *Adv. Funct. Mater.* **2014**, *24*, 5969.
[16] J. Smith, W. Zhang, R. Sougrat, K. Zhao, R. Li, D. Cha, A. Amassian, M. Heeney, I. McCulloch, T. D. Anthopoulos, *Adv. Mater.* **2012**, *24*, 2441.
[17] T. Uemura, Y. Hirose, M. Uno, K. Takimiya, J. Takeya, *Appl. Phys. Express* **2009**, *2*, 111501.
[18] T. Minari, M. Kano, T. Miyadera, S. D. Wang, Y. Aoyagi, K. Tsukagoshi, *Appl. Phys. Lett.* **2009**, *94*, 093307.
[19] S. Kwon, J. Kim, G. Kim, K. Yu, Y.-R. Jo, B.-J. Kim, J. Kim, H. Kang, B. Park, K. Lee, *Adv. Mater.* **2015**, *27*, 6870.
[20] Y. Yuan, G. Giri, A. L. Ayzner, A. P. Zoombelt, S. C. B. Mannsfeld, J. Chen, D. Nordlund, M. F. Toney, J. Huang, Z. Bao, *Nat. Commun.* **2014**, *5*, 3005.
[21] F. G. del Pozo, S. Fabiano, R. Pfattner, S. Georgakopoulos, S. Galindo, X. Liu, S. Braun, M. Fahlman, J. Veciana, C. Rovira, X. Crispin, M. Berggren, M. Mas-Torrent, *Adv. Funct. Mater.* **2016**, *26*, 2379.
[22] S. Georgakopoulos, F. G. del Pozo, M. Mas-Torrent, *J. Mater. Chem. C* **2015**, *3*, 12199.
[23] N. Crivillers, N. S. Oxtoby, M. Mas-Torrent, J. Veciana, C. Rovira, *Synthesis* **2007**, *11*, 1621.
[24] R. Pfattner, M. Mas-Torrent, C. Moreno, J. Puigdollers, R. Alcubilla, I. Bilotti, E. Venuti, A. Brillante, V. Laukhin, J. Veciana, C. Rovira, *J. Mater. Chem.* **2012**, *22*, 16011.
[25] R. Pfattner, M. Mas-Torrent, I. Bilotti, A. Brillante, S. Milita, F. Liscio, F. Biscarini, T. Marszalek, J. Ulanski, A. Nosal, M. Gazicki-Lipman, M. Leufgen, G. Schmidt, W. M. Laurens, V. Laukhin, J. Veciana, C. Rovira, L. W. Molenkamp, V. Laukhin, J. Veciana, C. Rovira, *Adv. Mater.* **2010**, *22*, 4198.
[26] L. Qiu, J. A. Lim, X. Wang, W. H. Lee, M. Hwang, K. Cho, *Adv. Mater.* **2008**, *20*, 1141.
[27] B. R. Hamilton, J. Smith, S. Ogier, M. Heeney, J. E. Anthony, I. Mcculloch, J. Veres, D. D. C. Bradley, T. D. Anthopoulos, *Adv. Mater.* **2009**, *21*, 1166.
[28] L. Lyu, D. Niu, H. Xie, N. Cao, H. Zhang, Y. Zhang, P. Liu, Y. Gao, *J. Chem. Phys.* **2016**, *144*, 034701.
[29] R. Li, J. W. Ward, D. M. Smilgies, M. M. Payne, J. E. Anthony, O. D. Jurchescu, A. Amassian, *Adv. Mater.* **2012**, *24*, 5553.
[30] D. J. Gundlach, J. E. Royer, S. K. Park, S. Subramanian, O. D. Jurchescu, B. H. Hamadani, A. J. Moad, R. J. Kline, L. C. Teague, O. Kirillov, C. A. Richter, J. G. Kushmerick, L. J. Richter, S. R. Parkin, T. N. Jackson, J. E. Anthony, *Nat. Mater.* **2008**, *7*, 216.
[31] J. W. Ward, M. A. Loth, R. J. Kline, M. Coll, C. Ocal, J. E. Anthony, O. D. Jurchescu, *J. Mater. Chem.* **2012**, *22*, 19047.
[32] S. C. B. Mannsfeld, M. L. Tang, Z. Bao, *Adv. Mater.* **2011**, *23*, 127.
[33] O. D. Jurchescu, S. Subramanian, R. J. Kline, S. D. Hudson, J. E. Anthony, T. N. Jackson, D. J. Gundlach, *Chem. Mater.* **2008**, *20*, 6733.
[34] S. Subramanian, K. P. Sung, S. R. Parkin, V. Podzorov, T. N. Jackson, J. E. Anthony, *J. Am. Chem. Soc.* **2008**, *130*, 2706.
[35] J. E. Anthony, D. L. Eaton, S. R. Parkin, *Org. Lett.* **2002**, *4*, 15.
[36] T. Izawa, E. Miyazaki, K. Takimiya, *Adv. Mater.* **2008**, *20*, 3388.
[37] S. Colella, C. Ruzié, G. Schweicher, J.-B. Arlin, J. Karpinska, Y. Geerts, P. Samorì, *Chempluschem* **2014**, *79*, 371.
[38] G. Giri, E. Verploegen, S. C. B. Mannsfeld, S. Atahan-Evrenk, D. H. Kim, S. Y. Lee, H. a. Becerril, A. Aspuru-Guzik, M. F. Toney, Z. Bao, *Nature* **2011**, *480*, 504.
[39] J. Cho, T. Higashino, T. Mori, *Appl. Phys. Lett.* **2015**, *106*, 193303.
[40] T. Minari, Y. Kanehara, C. Liu, K. Sakamoto, T. Yasuda, A. Yaguchi, S. Tsukada, K. Kashizaki, M. Kanehara, *Adv. Funct. Mater.* **2014**, *24*, 4886.
[41] M. Mas-Torrent, S. Masirek, P. Hadley, N. Crivillers, N. S. Oxtoby, P. Reuter, J. Veciana, C. Rovira, A. Tracz, *Org. Electron.* **2008**, *9*, 143.

